Proceedings of the 28th IEEE
EMBS Annual International Conference
New York City, USA, Aug 30-Sept 3, 2006

3D Modeling of Patient-Specific Geometries of Portal Veins Using MR Images

Yan Yang, Stephanie George, Diego R. Martin,
Allen R. Tannenbaum and Don P. Giddens

Abstract— **In this note, we present an approach for developing patient-specific 3D models of portal veins to provide geometric boundary conditions for computational fluid dynamics (CFD) simulations of the blood flow inside portal veins. The study is based on MRI liver images of individual patients to which we apply image registration and segmentation techniques and inlet and outlet velocity profiles acquired using PC-MRI in the same imaging session. The portal vein and its connected veins are then extracted and visualized in 3D as surfaces. Image registration is performed to align shifted images between each breath-hold when the MRI images are acquired. The image segmentation method first labels each voxel in the 3D volume of interest by using a Bayesian probability approach, and then isolates the portal veins via active surfaces initialized inside the vessel. The method was tested with two healthy volunteers. In both cases, the main portal vein and its connected veins were successfully modeled and visualized.**

Index Terms— **Image registration, 3D image segmentation, MRI, patient-specific, CFD geometric models, liver, portal vein**

I. Introduction

Imaging-based computational fluid dynamics (CFD) blood flow simulations have been used to analyze the flow pattern inside important vessels such as the aorta, carotid arteries and coronary arteries; see [1], [2] and the references therein. Patient-specific models can be built in 3D using images provided by computed tomography (CT) or magnetic resonance imaging (MRI), and detailed flow features such as the velocity profiles and wall shear stress distributions have revealed interesting relationships between the flow pattern and disease formation in these vessels. However, such techniques have yet to be applied to the portal vein.

Portal hypertension (PH) is a possible complication of cirrhosis of the liver, and one of the leading causes of death in the United States. PH is a result of the altered hemodynamics (blood flow) in the liver. Some consequences of PH are an enlarged spleen, ascites (fluid accumulation in the abdomen), and varices (dilation of intra-abdominal veins that can lead to bleeding and death) [3]. Because of the clinical significance of PH, it is important that noninvasive methods be developed to detect PH early and to monitor its progression with advancing liver disease. There is little available detailed hemodynamic knowledge of the normal liver, and therefore departures in physiological hemodynamics that arise from disease are difficult to interpret. Our proposal is based on the hypothesis that a detailed analysis of liver hemodynamics in cirrhosis and PH will lead to a non-invasive methodology for disease monitoring. Currently, no accurate or reliable non-invasive clinical tests are available for this purpose, and liver biopsies are still considered necessary for staging of cirrhosis and monitoring of disease progression.

Previous hemodynamic studies have used a variety of imaging methods, the most common being Doppler ultrasound; see [4], [5], [6]. There has been little use of MRI in hemodynamics studies of the liver to date. Ultrasound is prone to a number of potential measurement errors and is not capable of reproducibly visualizing the entire portal vein and major branches. These characteristics significantly restrict the capability of using Doppler ultrasound for detailed flow modeling in relation to PH. We believe that MRI has the potential to yield a more precise evaluation which in turn should lead to a more reproducible assessment of cirrhosis in the clinical setting.

The present work focuses on the 3D patient-specific modeling of portal veins using MRI images. Image registration is performed on the original data to correct misalignment between MRI scans of each breath-hold when the images are acquired. Voxel classification and active surface techniques are employed to extract and visualize the portal veins. The reconstructed model provides geometric boundary conditions for a CFD simulation of the blood flow. However, the CFD analysis is beyond the scope of this present work. In addition, this study addresses the feasibility of modeling the portal venous system in normal subjects from MRI images as a first step towards non-invasive classification and monitoring of cirrhosis and portal hypertension in patients with chronic liver disease.

The remainder of this note is organized as follows: In Section II, we present our modeling method combining image registration and image segmentation; Section III shows the results of two healthy portal veins as 3D surfaces to demonstrate the potential of our proposed method; Section IV discusses this work and gives possible future directions.

II. Methodology

A. Preprocessing and Image Registration

In order to achieve a more accurate result, preprocessing of the original MRI data is necessary, with a special emphasis on image registration. The anatomical position of the liver is strongly affected by respiratory motion, therefore either

Yan Yang (yan.yang@gatech.edu), Stephanie George, Allen R. Tannenbaum (tannenba@ece.gatech.edu) and Don P. Giddens (don.giddens@coe.gatech.edu) are with the Department of Biomedical Engineering, Georgia Institute of Technology, Atlanta, GA USA 30332. Diego R. Martin is with the Department of Radiology, Emory University, Atlanta, GA USA

respiratory gating or a series of breath-hold scans must be used. If breath-hold scanning is used, a single breath-hold is usually not sufficiently long for the entire volume of interest to be scanned, and in this case, a series of breath-hold scans are performed to acquire adequate data. Although the series of scans are made as continuous as possible, misalignment may occur in two adjacent slices between two series of images. Figure 1(a) shows the effect of misalignment by overlapping two adjacent slices on top of each other. It is obvious that one vessel cross-section becomes two in this image.

To solve this problem, rigid registration is applied to two consecutive image series before image segmentation is performed. We adopted rigid registration for the reason that there is no significant nonlinear deformation presented in the images. Mean squared difference (MSD) is used as the image similarity measure:

$$MSD = \frac{1}{N}\sum_{i=1}^{N}(f(p_i) - g(p_i))^2, \quad (1)$$

where f, g are the intensities of pixel p_i in the two images to be aligned and N is the total number of pixels in each image [7].

A translation (t_x, t_y) and a rotation by angle θ are applied to the second image in order to minimize the MSD between the first image (the last image in the first breath-hold series) and the second image (the first image in the second breath-hold series). A gradient decent approach is used to solve for the parameters (t_x, t_y, θ) that minimize MSD. Figure 1(b) shows the result after registration, and the "ghosts" of Figure 1(a) have disappeared.

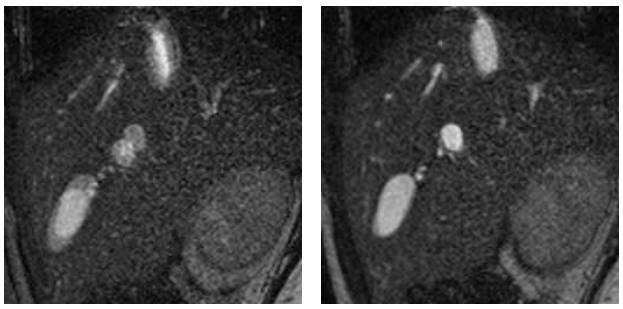

(a) **(b)**

Fig. 1. Before and after registration. (a) "Ghosts" appear between two overlapping adjacent slices before registration; (b) after registration.

After the registration, another preprocessing step is performed on the aligned data. MRI images usually have larger slice thickness than in-plane pixel spacing, so we linearly interpolate the data in the third direction (z-direction) to create near-isotropic voxels. This helps in generating smoother and more coherent 3D models of the veins.

B. Bayesian Voxel Classification Using EM

With the series of MRI scans properly aligned and interpolated in the z-direction, image segmentation is conducted to isolate the portal vein and its connected veins from the images. As opposed to the 2D registration, image segmentation is done in a 3D manner.

Given the intensity distributions of the MR images, we first perform a 3D voxel classification on the data. With the assumption that blood-filled regions exhibit higher intensities and the background exhibits lower intensities, we label each voxel with either "blood" or "background" by comparing the probability of a certain voxel belonging to blood or background. If the voxel has a higher probability of belonging to the blood, we label it as a blood voxel, otherwise we label it as a background voxel. In order to obtain the probabilities, we use the Bayes' rule [8], [9]:

$$Pr(\mathbf{x} \in c_k | V(\mathbf{x}) = v) = \frac{Pr(V(\mathbf{x}) = v | \mathbf{x} \in c_k) Pr(\mathbf{x} \in c_k)}{\sum_\gamma Pr(V(\mathbf{x}) = v | \mathbf{x} \in \gamma) Pr(\mathbf{x} \in \gamma)}, \quad (2)$$

which means that given the probability density function $p(V(\mathbf{x})|c_k)$ of each class c_k (blood or background) and the prior probability $Pr(\mathbf{x} \in c_k)$ of each class, posterior probabilities can be calculated via the Bayes' rule (2) to give the probabilities of a single voxel at position $\mathbf{x} = (x, y, z)$ belonging to different classes. $V(\mathbf{x})$ is the intensity of voxel $\mathbf{x}$, and v is any possible value within the range of the intensity in the images.

To determine the probability density functions for both blood and background, we analyze the histogram of the images using the expectation maximization (EM) method [10]. We assume that the histogram is a mixture of Gaussian functions (which is consistent with the noise model of MRI), and by using EM we learn the mean (μ_c), standard deviation (σ_c) and the weight (w_c) of each class. A k-means clustering of down-sampled voxels within the volume of interest is performed to initialize the EM process. Then the probability density function can be approximated using Gaussian functions with the learned mean and standard deviation in each class, which implies that the likelihood of a particular voxel having a certain intensity value v given that it is in class $c \in$ {blood, background} is:

$$Pr(V(\mathbf{x}) = v | \mathbf{x} \in c) = \frac{1}{\sqrt{2\pi}\sigma_c} \exp(-\frac{(v - \mu_c)^2}{2\sigma_c^2}), \quad (3)$$

The prior probability $Pr(\mathbf{x} \in c)$ that a particular voxel belongs to a certain class (blood or background) is determined by the weights w_c learned through EM.

The voxels can then be labeled according to the *maximum a posteriori* (MAP) rule:

$$C(\mathbf{x}) = \arg \max_{c \in \{blood, background\}} Pr^*(\mathbf{x} \in c | V(\mathbf{x}) = v), \quad (4)$$

where $C(\mathbf{x})$ is the class that voxel $\mathbf{x}$ belongs to, and Pr^* is a smoothed version of the posterior probability obtained using the anisotropic smoothing [11] described by the following affine invariant flow:

$$\frac{\partial Pr}{\partial t} = \text{sign}(H)\kappa_+^{1/4}\vec{N}, \quad (5)$$

where H and κ are the mean curvature and Gaussian curvature of Pr, and $\kappa_+ := \max\{\kappa, 0\}$. $\vec{N}$ is the inward unit normal. Details about the justification of this "knowledge-based" segmentation method may be found in [8], [9].

Figure 2 shows two images overlaid with the voxel labeling result. The blood regions are shown as white, while other regions are the same as in the original images. All possible blood-filled regions are labeled as white in these images, including the portal vein and other blood vessels inside the volume. Note that the voxel labeling is performed in 3D and the 2D slices are only shown to demonstrate the result.

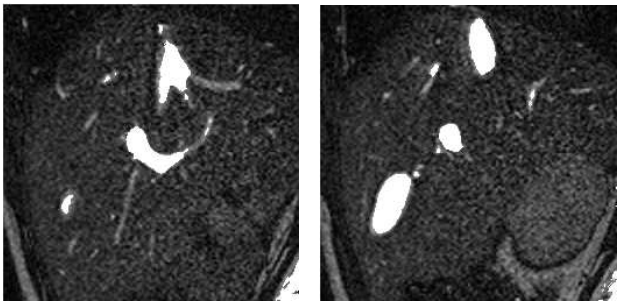

(a) **(b)**

Fig. 2. Voxel labeling result. White regions are blood-filled regions. (a) Slice #10 of the 3D data; (b) Slice #19.

C. Isolating Portal Veins Using Active Surfaces

The results obtained through voxel labeling identify all high intensity regions as blood-filled regions. These regions, however, contain several other vessels in addition to the object of interest, i.e., the portal vein. Thus a further step is needed to extract and isolate the portal vein and its connected veins from the voxel labeling results.

We extract the portal vein by expanding a balloon from the interior of the vessel via the use of a certain active surface model which extends the approach of [12], [13] and is implemented by level sets [14], [15]:

$$\frac{\partial \psi}{\partial t} = g(\nabla I)(H + c)\|\nabla \psi\| + \nabla \psi \cdot \nabla g(\nabla I). \qquad (6)$$

Here $\psi(x, y, z, t)$ is the level set function with its zero level set representing the propagating surface, and $g(\nabla I)$ is a stopping term based on image gradient that slows down the surface evolution when near an edge. Further, H is the mean curvature of the propagating surface (which preserves smoothness), and c is an adaptive propagation term that determines the direction of the evolving surface by evaluating the probability of the voxels residing on the current surface. If the probability is larger for belonging to the blood region, the surface will continue to expand, otherwise it will shrink to capture the boundary of the portal vein.

The balloon expansion process is initialized by placing a small bubble inside the portal vein, and the active surface grows to capture the veins of interest while leaving out other high intensity regions. The resulting surface is smooth due to the curvature term and gives sub-voxel resolution by obtaining the zero level set of ψ. Figure 3 shows four slices including the two slices shown in Figure 2, but only the portal vein in the center of the images is captured (with a white contour around it).

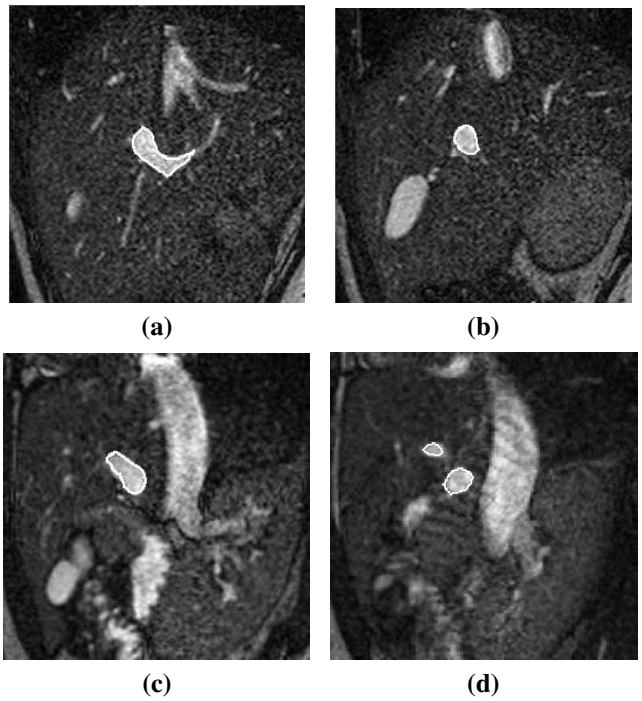

(a) **(b)** **(c)** **(d)**

Fig. 3. Segmentation results shown in 2D: original images overlaid with contours. (a) Slice #10; (b) Slice #19; (c) Slice #27; (d) Slice #33.

III. Results

In this section we present the 3D results obtained using our modeling method. The MRI data were acquired using the Philips 1.5T Intera system equipped with a 4-element body phased array coil on two healthy volunteers without liver problems. Both subjects were imaged using balanced fast field echo (BFFE) scans, with a field of view of 300mm (subject #1) and 330mm (subject #2), matrix reconstructed size to 256, slice thickness and spacing of 3mm, and in-plane resolution of 1mm$\times$1mm. The first subject was respiratory gated and the second one was a series of breath-hold scans, which required image registration to align the series.

Figure 4 shows the two reconstructed surfaces with the veins of interest labeled: portal vein (PV), right portal vein (RPV), left portal vein (LPV), splenic vein (SV) and superior mesenteric vein (SMV).

IV. Discussion and Conclusions

In this note, we presented an approach that allows the construction of 3D patient-specific models of portal veins using MRI images to provide geometric boundary conditions for CFD blood flow simulations. Image registration and segmentation methods are developed to effectively register misaligned MRI data and automatically extract the portal veins. The proposed method was tested on two healthy

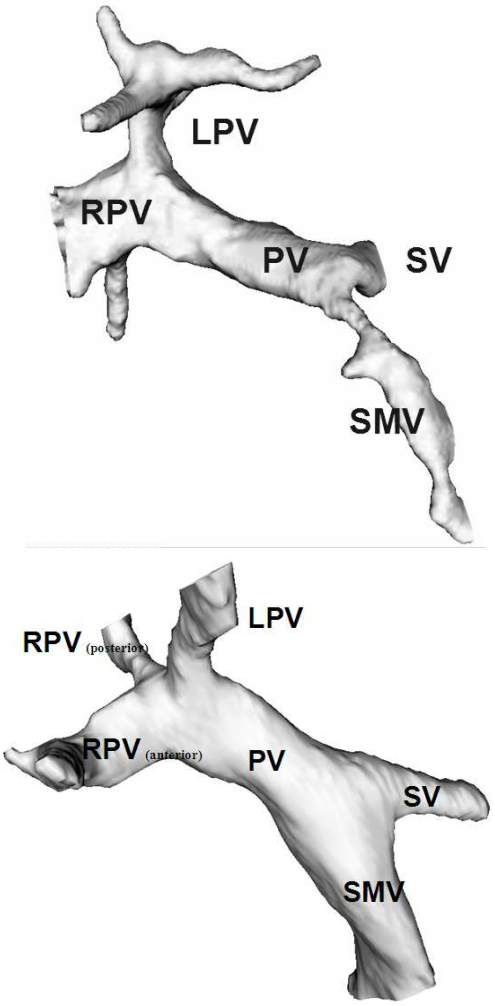

Fig. 4. 3D surface rendering of two reconstructed models of the portal vein and its connected veins. PV: Portal Vein, RPV: Right Portal Vein, LPV: Left Portal Vein, SV: Splenic Vein, SMV: Superior Mesenteric Vein.

subjects with the portal vein and its connected veins successfully modeled. The 3D segmentation approach that utilizes the active surface models brings natural smoothness to the results. A preliminary validation was conducted by inviting a radiologist to identify the segmented vein branches, and quantitative validations will be further carried out by comparing the machine segmentation results with manual segmentations provided by medical experts.

Geometric models provide only partial boundary conditions for CFD simulations. Beside the geometry, inlet and outlet velocity boundary conditions should also be provided. We acquire these by using phase contrast (PC)-MRI during the same imaging session of the geometry scan using the same MRI scanner. Dynamic velocity profiles at interested cross-sections of the veins can then be obtained from the PC-MRI data.

Finally, for a comparative analysis and further study, patients with portal hypertension will also be imaged using MRI, from which 3D models will be built for our CFD simulations.

V. Acknowledgements

This work is part of the National Alliance for Medical Image Computing (NAMIC) funded through the NIH Roadmap for Medical Research, Grant U54 EB005149. It was also funded by NIH NAC grant P41 RR-13218.

References

[1] Steinmen DA, "Image-Based Computational Fluid Dynamics Modeling in Realistic Arterial Geometries", *Annals of Biomedical Engineering*, **30** (2002) pp. 483-46.

[2] Suo J, Yang Y, Oshinski J, Tannenbaum AR, Gruden J, and Giddens DP, "Flow Patterns and Wall Shear Stress Distributions at Atherosclerotic-Prone Sites in a Human Left Coronary Artery - An Exploration Using Combined Methods of CT and Computational Fluid Dynamics", in *Proc. IEEE EMBS* (2004) pp. 3789-3791.

[3] Thomson A and Shaffer E, *First Principles of Gastroenterology: The Basis of Disease and an Approach to Management, 3rd edition*, University of Toronto Press, 1992.

[4] Kayacetin E, Efe D, and Dogan C, "Portal and splenic hemodynamics in cirrhotic patients: relationship between esophageal variceal bleeding and the severity of hepatic failure", *Journal of Gastroenterology*, **39 (7)** (2004) pp. 661-667.

[5] Kutlu R, Karaman I, Akbulut A, Baysal T, Sigirci A, Alkan A, Aladag M, Seckin Y, and Sarac K, "Quantitative Doppler evaluation of the splenoportal venous system in various stages of cirrhosis: differences between right and left portal veins", *Journal of Clinical Ultrasound*, **30 (9)** (2002) pp. 537-543.

[6] Vyas K, Gala B, Sawant P, Das HS, Kulhalli PM, and Mahajan SS, "Assessment of portal hemodynamics by ultrasound color Doppler and laser Doppler velocimetry in liver cirrhosis", *Indian Journal of Gastroenterology*. **21 (5)** (2002) pp. 176-178.

[7] Holden M and Hill DLG, *et al*. "Voxel Similarity Measures for 3-D Serial MR Brain Image Registration", *IEEE Trans. Medical Imaging*, **19 (2)** (2000) pp. 94-102.

[8] Haker S, Sapiro G, and Tannenbaum AR, "Knowledge-Based Segmentation of SAR Data with learned Priors", *IEEE Tran. on Image Processing,* **9** (2000), pp. 298-302.

[9] Yang Y, Tannenbaum AR, and Giddens DP, "Knowledge-Based 3D Segmentation and Reconstruction of Coronary Arteries Using CT Images", *In Proceedings of the 26th Annual International Conference of the IEEE EMBS*, (2004) pp. 1664-1666.

[10] D'Souza AA, "Using EM (Expectation Maximization) to Estimate a Probability Density with a Mixture of Gaussians", *http://wwwclmc.usc.edu/ãdsouza/notes/mix_gauss.pdf*

[11] Olver P, Sapiro G, and Tannenbaum A, "Invariant geometric evolutions of surfaces and volumetric smoothing", *SIAM J. Applied Math.* **57** (1997), pp. 176-194.

[12] Kichenassamy S, Kumar A, Olver P, Tannenbaum A, and Yezzi A, "Conformal curvature flows: from phase transitions to active vision," *Archive for Rational Mechanics and Analysis* **134** (1996), pp. 275-301.

[13] Caselles V, Kimmel R, and Sapiro G, "Geodesic snakes," *Int. J. Computer Vision* **22** (1997), pp. 61-79.

[14] Osher S and Fedkiw R, *Level Set Methods and Dynamic Implicit Surfaces*, Springer-Verlag, 2003.

[15] Sethian JA, *Level Set Methods and Fast Marching Methods*, Cambridge University Press, 1999.